Z. Cao, J. Zhang, L. Xiang, and X. Ge, "Outage Probability Analysis of Multi-Connectivity in UAV-Assisted Urban mmWave Communications," accepted for presentation in *IEEE International Symposium on Personal, Indoor and Mobile Radio Communications (PIMRC)*, Valencia, Spain, Sep. 2024.

Outage Probability Analysis of Multi-Connectivity in UAV-Assisted Urban mmWave Communications

Zhengxin Cao[1], Jing Zhang[1], Lin Xiang[2], and Xiaohu Ge[1]
[1]Huazhong Uni. Science and Technology, [2]Technische Universität Darmstadt
Emails:{zhengxincao,zhangjing,xhge}@hust.edu.cn, l.xiang@nt.tu-darmstadt.de

***Abstract*—Unmanned aerial vehicle (UAV)-assisted millimeter-wave (mmWave) communication presents a promising solution for high data-rate wireless applications in urban environments. However, due to limited energy supply and communication capability, UAVs can only provide temporary communication services. This challenge motivates the exploration of three-dimensional (3D) integrated aerial and ground mmWave communications utilizing the multi-connectivity (MC) technique. By leveraging both ground and aerial mmWave links over licensed and unlicensed mmWave spectrums, respectively, the MC technique can effectively exploit spatial and frequency diversity to enhance the connectivity and reliability of UAV-assisted mmWave communications. We develop a unified framework based on stochastic geometry and Markov chain to analyze the coverage and outage probabilities of the 3D integrated aerial/ground mmWave networks. Furthermore, we show that an optimal UAV flight altitude for maximizing the coverage probability of UAV communication exists and derive it in a closed-form expression. Simulation results demonstrate that UAVs can maintain reliable mmWave connections even when connections from terrestrial mmWave base stations (BSs) are obstructed by buildings, underscoring the benefits of MC in enhancing the robustness of 3D integrated aerial and ground mmWave networks.**

I. Introduction

Millimeter-wave (mmWave) communication is an advanced physical-layer technology designed to enable ultra high-capacity low-latency wireless access in the sixth-generation (6G) wireless networks. By utilizing the extensive licensed and unlicensed mmWave spectrum, this technology is expected to satisfy the stringent latency and throughput requirements of bandwidth-intensive 6G applications such as virtual/augmented reality (VR/AR) and holographic telepresence [1], [2]. However, the deployment of mmWave communications in complex environments, e.g., in urban areas, presents unique challenges. Particularly, high-frequency mmWave signals experience significant path losses and are susceptible to obstructions from urban infrastructure. Such obstructions can drastically impair the reliability of urban mmWave communication systems and disrupt mmWave-based services.

Recently, aerial base stations (BSs) enabled by unmanned aerial vehicles (UAVs) have emerged as a promising solution to enhance the reliability of mmWave signal transmission [3]. In practice, elevated UAVs can establish strong line-of-sight (LoS) connections with ground user equipments (UEs) with a high likelihood, and flexibly reposition themselves to maintain this LoS communication, even in urban areas. As such, it provides a favorable solution for mitigating the non-line-of-sight (NLoS) scenarios typical in terrestrial mmWave networks [4]. The spectrum efficiency of mmWave aerial BSs was evaluated in [4]. Additionally, terrestrial mmWave BS deployed atop buildings can also enhance the likelihood of LoS connections. The blockage effect of buildings was modeled in [5] using cylinders to evaluate the impact of BS height on the downlink coverage probability of mmWave BSs. Compared with those placed on the ground at fixed heights, mmWave BSs deployed on buildings can better mitigate the obstruction of buildings on signal transmission [5].

Despite the advances in [3]–[5], comprehensive performance analysis of UAV-assisted 3D mmWave wireless networks that accounts for the spatial characteristics of urban environments and incorporates the height of UAV within a unified three-dimensional (3D) spatial model, is still lacking in the existing literature. Furthermore, although high altitudes of the UAV and mmWave BSs can increase the likelihood of LoS connections, essential for mmWave communication, they also cause high propagation path loss, potentially reducing the resulting achievable data rates. Additionally, UAVs are usually constrained in size, weight, and power (SWAP), which severely restricts their operation time. In contrast, mmWave BSs mounted on buildings can provide sustainable long-term service. Given these factors, the joint impact of UAV flight altitude and mmWave BS heights on the overall system performance presents a critical area for further research but has not been investigated in the exiting literature yet.

To address the identified research gaps, this paper introduces a unified modeling framework that leverages stochastic geometry to accurately capture the spatial locations of ground BSs, UAV, and urban buildings in UAV-assisted 3D mmWave networks. Unlike existing research on UAV-assisted mmWave communications, our study focuses on enabling effective mmWave communications within urban environments. This primarily involves communication within the 3D region defined by the LoS clearance zones between the UEs and their serving BSs. Additionally, we incorporate the multi-connectivity (MC) technique to enhance the synergy between ground-based and UAV-aided mmWave communications [6]. Leveraging the analytical tractability of the proposed framework, we characterize the coverage probabilities of both the ground BSs and the UAV, which follows a predetermined flight path. Based on these results, we further evaluate the outage probabilities for UEs utilizing the MC technique. Our contributions are as follows:

- We propose a unified framework for modeling the 3D spatial and temporal characteristics of UAV-assisted urban mmWave communications within LoS clearance zones of UEs and BSs. We employ this framework to evaluate the connectivity and reliability of mmWave links via analyzing the coverage and outage probabilities, respectively.
- We derive a closed-form expression for the optimal UAV flight altitude, which maximizes the coverage probability, while taking into consideration the UAV's communication range and the 3D spatial distribution of urban buildings.
- By employing the Markov chain, we demonstrate that UEs equipped with large size of buffers can significantly benefit

The work is supported by the National Natural Science Foundation of China (No.U2001210), the National Key Research and Development Program of China (No.2020YFB1806605). The work of L. Xiang has been funded by the LOEWE initiative (Hesse, Germany) within the emergenCITY center under grant LOEWE/1/12/519/03/ 05.001(0016)/72 and has been supported by the BMBF project Open6GHub under grant 16KISKO14.

from the MC technique. Particularly, they can exploit both UAV-aided and ground-based mmWave communications to significantly improve the connectivity and reliability of the integrated system.

In the remainder of this paper, the system model is presented in Section II. The optimal flight altitude for the UAV to maximize its coverage probability is derived in Section III. In Section IV, the outage probability of MC UAV-assisted mmWave communication is analyzed utilizing a 2D Markov chain. In Section V, we evaluate the performance of the UAV-assisted mmWave communication system and conclude the paper in Section VI.

II. System Model

A. Network Model

As shown in Fig. 1, we consider downlink communication in a UAV-assisted mmWave network in an urban area. The mmWave BSs consist of both the movable BS enabled by a rotary-wing UAV and the ground BSs. The UEs are randomly distributed on the ground and their 2D locations, denoted as Φ_{UE}, follow a homogeneous Poisson Point Process (PPP) with density λ_{UE}. The ground mmWave BSs are distributed over the area to provide long-term access services for the UEs. For mathematical tractability, we assume that the 2D locations of the BSs, denoted by Φ_{BS} with density λ_{BS}, independent of Φ_{UE}. The altitudes of the UEs are fixed as H_{UE}.

Due to weak diffraction and penetration capabilities of mmWave signals, buildings situated between the UEs and the ground BSs can significantly attenuate mmWave signal propagation and disrupt the downlink communication. The buildings are centered at 2D locations, denoted by Φ_{BU}, and we assume that Φ_{BU} follows a PPP with density λ_{BU}, independent of Φ_{BS} and Φ_{UE}. Meanwhile, we assume that the heights, lengths, and widths of the buildings follow independent uniform distributions in the ranges of $(\mathbb{E}[H]-h_0, \mathbb{E}[H]+h_0)$, $(\mathbb{E}[L]-l_0, \mathbb{E}[L]+l_0)$, and $(\mathbb{E}[W]-w_0, \mathbb{E}[W]+w_0)$, where $\mathbb{E}[H]$, $\mathbb{E}[L]$, and $\mathbb{E}[W]$ are the expected height, length, and width of the buildings, respectively [7]. In this paper, we assume that $\mathbb{E}[H]$, $\mathbb{E}[L]$, $\mathbb{E}[W]$, h_0, l_0, and w_0 are given *a priori*. Moreover, the mmWave BSs are deployed atop part of the buildings, whereby the height of the mmWave BSs H_{BS} follows a uniform distribution in the range of $(\mathbb{E}[H]-h_0, \mathbb{E}[H]+h_0)$.

To mitigate the blockage effect caused by the buildings, the UAV serves as a temporary mobile BS by flying over a circular trajectory $\mathcal{Q}$ with a radius R_{U} and a constant height H_{U}. We assume that the UAV and ground BSs implement mmWave communications exploiting the MC technique. Thereby, the UAV and the ground BSs simultaneously serve the UEs over an unlicensed and a licensed mmWave spectrum, respectively. Specially, the licensed spectrum is shared by the ground BSs. As a result, the communications between the UEs and their serving ground BSs can be interfered by other ground BSs. However, the communications between the UEs and the UAV are not interfered by the ground BSs.

B. Channel Model for LoS mmWave Transmission

We assume that the UEs can establish a connection with the UAV or a mmWave BS, provided no blockage/building exists in the LoS clearance zone [8]. In this case, the mmWave signal can propagate over a LoS link, without being obstructed by any blockage. This assumption is made due to the fact that mmWave signals are highly sensitive to blockages in the urban

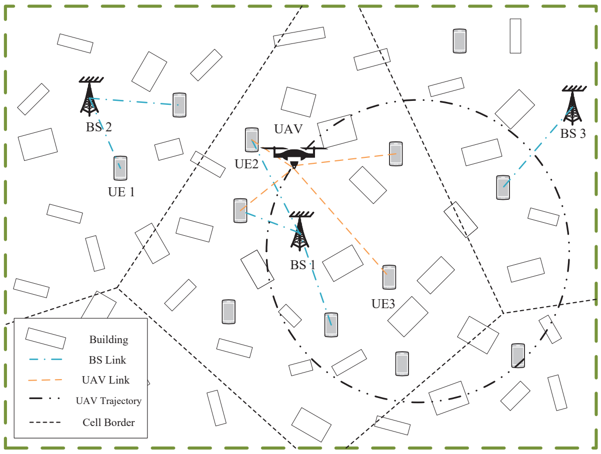

Fig. 1. System model.

environment. That is, mmWave signals would be significantly attenuated over a NLoS link, for which the NLoS propagation of mmWave signals is not considered in this paper. This implies that only the mmWave BSs distributed in the LoS clearance region of a user can send signals to the user. Thus, the locations of unblocked mmWave BSs follow a PPP distribution refined by the LoS clearance zone.

Without loss of generality, we take the UE located at x_0 as the *typical* UE and its serving BSs include a ground BS located at y_{B_0} and the UAV located at y_{U}. In the following, we only illustrate the LoS clearance zones for the serving ground BS. The case of the UAV can be just modeled in the same manner. In particular, to characterize the LoS clearance zones between the typical UE and its serving ground BS, we set a 3D Cartesian coordinate system with the origin O located in the middle of the typical UE and the serving BS. Meanwhile, the xOy plane is placed on the horizontal plane such that the z-axis is pointed towards the sky while being perpendicular to the xOy plane. The Euclidean distance between the UE and the serving BS can be calculated as $r = \|x_0 - y_{\mathrm{B}_0}\|$. The horizontal distance between the UE and the serving BS in the xOy plane is given by $d = \sqrt{r^2 - h_{\mathrm{BS}}^2}$, where $h_{\mathrm{BS}} = H_{\mathrm{BS}} - H_{\mathrm{UE}}$ is the height difference between the UE and the serving BS. The elevation angle of the serving BS for xOy plane, denoted by φ, can be calculated as $\varphi = \cos^{-1}(d/r)$. Then, the LoS clearance zone can be captured by [9]

$$\frac{x^2}{b^2} + \frac{(y\cos\varphi - z\sin\varphi)^2}{a_0^2} + \frac{(y\sin\varphi + z\cos\varphi)^2}{b^2} \le 1, \quad (1)$$

where $a_0 = \frac{r}{2} + \frac{\lambda_f}{4}$, $b = \eta\sqrt{\frac{r\lambda_f}{4} + \frac{\lambda_f^2}{16}}$, λ_f is the carrier wavelength and η is the minimum ratio of the clearance for the first Fresnel zone.

The mmWave wireless channels are impaired by both large-scale and small-scale fading. Assume that the ground BSs have the transmit power $P_{t,b}$. The received power at the typical UE can be modeled as

$$P_r = P_{t,b} H_{x_0, y_{\mathrm{B}_0}} L^{-1}(x_0, y_{\mathrm{B}_0}), \quad (2)$$

where $L(x_0, y_{\mathrm{B}_0}) = S_{x_0, y_{\mathrm{B}_0}} \|x_0 - y_{\mathrm{B}_0}\|^{\alpha}$ is the large-scale attenuation introduced by path loss. In particular, $S_{x_0, y_{\mathrm{B}_0}}$ denotes the shadowing effect, α is the path loss exponent, and

$\|x_0 - y_{\mathrm{B}_0}\|$ is the Euclidean distance between the UE and the serving ground BS. We model the small-scale fading $H_{x,y}$ over the mmWave link as a Nakagami random variable [10], i.e., $H_{x_0,y_{\mathrm{B}_0}} \sim \mathrm{Gamma}\,(m,1)$, where m is the Nakagami fading parameter. On the other hand, let $P_{t,u}$ and $h_{\mathrm{U}} = H_{\mathrm{U}} - H_{\mathrm{UE}}$ be the transmit power of the UAV and the height difference between the UE and the UAV, respectively. The channel model for the UAV can be similarly obtained as in (2).

C. Queue Model

At the UE receiver, the signal-to-interference-plus-noise ratio (SINR) of the desired signal received from the serving ground BS located at y_{B_0} is given as

$$\mathrm{SINR}_{\mathrm{BS}} = \frac{H_{x_0,y_{\mathrm{B}_0}} L^{-1}\left(x_0, y_{\mathrm{B}_0}\right)}{\frac{N_0}{P_{t,b}} + \sum\limits_{\mathrm{B}_i \in \Phi_{\mathrm{BS}} \setminus \{\mathrm{B}_0\}} H_{x_0,y_{\mathrm{B}_i}} L^{-1}\left(x_0, y_{\mathrm{B}_i}\right)}, \tag{3}$$

where N_0 is the thermal noise power at the UE. Note that the desired signal received at the typical UE from its serving ground BS in the LoS clearance zone may suffer from severe interference from other ground BSs. Meanwhile, since the mmWave signals from the UAV is not interfered by the ground BSs, the signal-to-noise ratio (SNR) at the typical UE when it is served by the UAV is given as

$$\mathrm{SNR}_{\mathrm{UAV}} = \frac{P_{t,u} H_{x_0,y_{\mathrm{U}}} L^{-1}\left(x_0, y_{\mathrm{U}}\right)}{N_0}. \tag{4}$$

Note that although the ground BSs and the UAV can connect and transmit mmWave signals to the UE when they are located within the LoS clearance zone characterized by (1), the data packets are successfully decoded at the UE only if the receiving S(I)NR exceeds an predefined SINR threshold, denoted by T. The coverage probabilities of the serving ground BS and the UAV, denoted by $P_{c,\mathrm{BS}}(T)$ and $P_{c,\mathrm{UAV}}(T)$, respectively, are defined as the probabilities that the serving BS is located within the LoS clearance zone for the typical UE and that the UE's S(I)NR exceeds T.

On the other hand, each UE is equipped with a buffer of finite size C to temporarily cache the successfully decoded packets received from the ground BSs or the UAV, before they are further fetched and processed by the application layer. We assume that both the ground BSs and the UAV transmit the packets at the same rate λ. The corresponding packet arrival rates at the typical UE is given by $\lambda_b = \lambda P_{c,\mathrm{BS}}(T)$ and $\lambda_u = \lambda P_{c,\mathrm{UAV}}(T)$, respectively. For the packets cached in the buffer, the UE fetches the decoded packets with a fixed packet service rate μ. Note that once the UE's buffer becomes full, the newly arrived data packets, transmitted from the ground BSs or the UAV, will be discarded, even if the LoS connectivity is available and the SINR exceeds the threshold.

D. System Performance Metrics

By employing the MC technique for mmWave signal transmission, the UE can exploit the connectivity provided by both the UAV and the ground BSs to enhance the reception of data packets. For a comprehensive performance evaluation, we will analyze the connectivity and the reliability of mmWave links via the UE coverage probability of the MC mmWave system and the outage probability of data communication, respectively.

1) Coverage Probability P_c: The total coverage probability of UEs employing the MC technique is given as $P_c = 1 - \left(1 - P_{c,\mathrm{BS}}\left(T\right)\right)\left(1 - P_{c,\mathrm{UAV}}\left(T\right)\right)$.
2) Outage Probability P_{out}: Let Π_C be the probability that the UE buffer becomes full. When the buffer is full, the newly arrived packets are dropped and the UE is in outage. The outage probability is defined as $P_{out} = 1 - P_c\left(1 - \Pi_C\right)$, where $P_c\left(1 - \Pi_C\right)$ is the probability that the UE can connect to the ground BSs or UAV and that the UE's buffer is not full.

III. Analysis of Coverage Probabilities

In this section, we first analyze in Section III-A the probabilities of establishing a LoS mmWave link from the typical UE to its serving BSs at a distance of r away, taking into account the 3D spatial distributions of the UEs, BSs, and buildings. We further derive the distance distribution of the LoS links from the ground BSs and the flying UAV to the typical UE . Based on these derived results, we then evaluate the coverage probabilities of both ground BSs and the UAV in Section III-B.

A. Distance Distribution of LoS mmWave Links

The following lemma characterizes the probability of having a LoS mmWave link within given distance x.

Lemma 1. In the considered 3D urban environment, the LoS probability of the serving UAV or ground BS, namely the probability that no building exists in the LoS clearance zone of the typical UE, is given as [9]

$$P_s^{\mathrm{LoS}}(x) = \exp\left(-\lambda_{\mathrm{BU}}\left(\frac{\sqrt{x^2 - h_s^2}}{\pi h_s}\mathbb{E}[S_{sa}] + \mathbb{E}[S_{ta}]\right)\right), \tag{5}$$

where $s \in \{\mathrm{UAV}, \mathrm{BS}\}$, h_s is the height difference between the UE and the ground BS or the UAV defined in Section II-B, λ_{BU} is the density of building distribution, and $\mathbb{E}[S_{sa}] = 2\mathbb{E}[H]\left(\mathbb{E}[W] + \mathbb{E}[L]\right)$ and $\mathbb{E}[S_{ta}] = \mathbb{E}[W]\mathbb{E}[L]$ are the average side area and bottom area of the buildings, respectively.

Proof: The proof follows from [9] and is ignored herein due to page limitation. ■

Let $f_s^{\mathrm{LoS}}\left(x\right), s \in \{\mathrm{BS}, \mathrm{UAV}\}$ be the probability density function (PDF) of distance from the UE to its serving ground/aerial BS when both are in the LoS clearance zone, where x denotes the distance of the LoS link between the UE and its serving BS. In the following lemma, we derive the PDF of the distance from the UE to the serving ground BS.

Lemma 2. The probability that the typical UE has at least one BS for LoS communication is given by $B_L = 1 - \exp\left(-2\pi\lambda_{\mathrm{BS}}\int_0^\infty rP_{\mathrm{BS}}^{\mathrm{LoS}}\left(r\right)\mathrm{d}r\right)$. Moreover, given that the typical UE observes at least one ground BS for establishing LoS links, the conditional PDF of the distance between the typical UE and the nearest of these BSs is given by

$$\begin{aligned} f_{\mathrm{BS}}^{\mathrm{LoS}}(x) &= 2\pi\lambda_{\mathrm{BS}}\sqrt{x^2 - {h_{\mathrm{BS}}}^2}P_{\mathrm{BS}}^{\mathrm{LoS}}\left(x\right) \\ &\times \exp\left(-2\pi\lambda_{BS}\int_0^x rP_{\mathrm{BS}}^{\mathrm{LoS}}\left(r\right)\mathrm{d}r\right)/B_L, \quad x > 0. \end{aligned} \tag{6}$$

Proof: The proof follows [7] and is omitted here due to the limited page space. ■

In this paper, we assume that the UAV flies with random speeds [3]. Hence, despite the fixed flight trajectory, the positions of the UAV are not predictable at the typical UE. Moreover, the service time of the UAV is also random. Due to the random flying speeds and service time of the UAV, we assume that the locations of the UAV when serving the

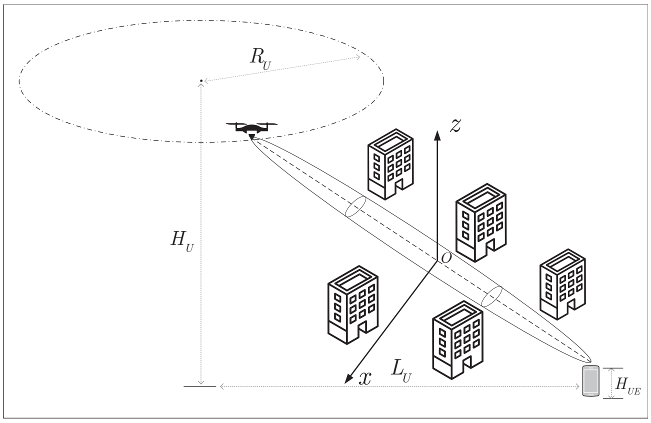

Fig. 2. UAV Distance Analysis.

UE are uniformly distributed on its trajectory. Let L_U be the horizontal distance between the typical UE and the center of the flight trajectory/circle, cf. Fig. 2. Then, the PDF of the distance between the UAV and the typical UE is given in the following proposition.

Proposition 1. The PDF of the distance between the UE and the UAV located in the LoS clearance zone of the UE is

$$f_{\mathrm{UAV}}^{\mathrm{LoS}}(x)=\frac{2x\exp\left(\frac{-\lambda_{\mathrm{BU}}\mathbb{E}[S_{sa}]}{\pi h_{\mathrm{U}}}\sqrt{x^2-h_{\mathrm{U}}^2}-\lambda_{\mathrm{BU}}\mathbb{E}[S_{ta}]\right)}{\pi\sqrt{(l_{\mathrm{U,max}}^2-x^2)(x^2-l_{\mathrm{U,min}}^2)}}. \quad (7)$$

Proof: The cumulative distribution function of the distance between the UE and the UAV can be derived as

$$F_{\mathrm{UAV}}(x)=\frac{1}{\pi}\cos^{-1}\frac{R_{\mathrm{U}}^2+L_{\mathrm{U}}^2+h_{\mathrm{U}}^2-x^2}{2R_{\mathrm{U}}L_{\mathrm{U}}}, \quad (8)$$

where $x\in[l_{\mathrm{U,min}},l_{\mathrm{U,max}}]$, $l_{\mathrm{U,min}}=\sqrt{(L_{\mathrm{U}}-R_{\mathrm{U}})^2+h_{\mathrm{U}}^2}$ and $l_{\mathrm{U,max}}=\sqrt{(L_{\mathrm{U}}+R_{\mathrm{U}})^2+h_{\mathrm{U}}^2}$ are the minimal and maximal distances between the UAV and the UE, respectively.

Hence, the PDF of the distance between the UAV and the UE is given by

$$f_{\mathrm{UAV}}(x)=\frac{\mathrm{d}F_{\mathrm{UAV}}(x)}{\mathrm{d}x}=\frac{1}{\pi}\frac{2x}{\sqrt{(l_{\mathrm{U,max}}^2-x^2)(x^2-l_{\mathrm{U,min}}^2)}}, \quad (9)$$

where $x\in(l_{\mathrm{U,min}},l_{\mathrm{U,max}})$.

Combining (5) and (9), we can derive the PDF of the distance between the UE and the UAV located in the LoS clearance zone of the UE as shown in (7). ■

B. Coverage Probabilities of Ground BSs and UAV

Based on the results in Sec. III-A, we further derive here the coverage probabilities of the ground BSs and the UAV, as well as the total coverage probability of the UE. We start with deriving the coverage probability of ground BSs conditioned on that the link distance is r. The result is given as

$$\begin{aligned}
&\mathbb{P}(\mathrm{SINR}_{\mathrm{BS}}>T\mid\|x_0-y_{\mathrm{B}_0}\|=r)\\
&=\mathbb{P}\left(H_{x,y_{\mathrm{B}_0}}>L(x_0,y_{\mathrm{B}_0})(TN_0/P_{t,b}+\sigma_I)\right)\\
&=\mathbb{E}_r\left(\mathbb{E}_I\left(\sum_{k=0}^{m}\frac{s^k}{k!}\sigma_I^k\exp(-s\sigma_I)\right)\right) \quad (10)\\
&=\mathbb{E}_r\left(\sum_{k=0}^{m}\frac{(-s)^k}{k!}\frac{d^k[\mathcal{L}_I(s)]}{ds^k}\right)\\
&=\mathbb{E}_r\left(\sum_{k=0}^{m}\frac{(-s)^k}{k!}\frac{d^k\left[\exp\left(-2\pi\lambda_{\mathrm{BS}}\int_{r^2}^{\infty}1-\left(\frac{m}{m+sTu^{-\alpha/2}}\right)^m du\right)\right]}{ds^k}\right),
\end{aligned}$$

where $\sigma_I=T\sum_{\mathrm{B}_i\in\Phi_{\mathrm{B}}\setminus\{\mathrm{B}_0\}}H_{x,y_{\mathrm{B}i}}L^{-1}(x_0,y_{\mathrm{B}i})$, $s=L(x_0,y_{\mathrm{B}0})$, and $\mathcal{L}_I(\cdot)$ is the Laplace transform of σ_I [11].

Based on (10), the coverage probability of the serving ground BS can be calculated as

$$\begin{aligned}
&P_{c,\mathrm{BS}}(T)=\int\mathbb{P}(\mathrm{SINR}_{\mathrm{BS}}>T\mid\|x_0,y_{\mathrm{B}0}\|=x)f_{\mathrm{BS}}^{\mathrm{LoS}}(x)\,\mathrm{d}x\\
&=\int_0^{\infty}\frac{2\pi\lambda_{\mathrm{BS}}\sqrt{x^2-h_{\mathrm{BS}}^2}P_{\mathrm{BS}}^{\mathrm{LoS}}(x)\,\mathrm{e}^{-2\pi\lambda_{\mathrm{BS}}\int_0^x rP_{\mathrm{BS}}^{\mathrm{LoS}}(r)\mathrm{d}r}}{B_L}\cdot\\
&\sum_{k=0}^{m}\frac{(-s)^k}{k!}\frac{\mathrm{d}^k}{\mathrm{d}s^k}\left[\exp\left(-2\pi\lambda_{\mathrm{BS}}\int_{r^2}^{\infty}1-\left(\frac{m}{m+sTu^{-\alpha/2}}\right)^m du\right)\right]\mathrm{d}x. \quad (11)
\end{aligned}$$

As both the UAV's location and the time of user access are random, we analyze the coverage probability of the UAV by averaging along its entire trajectory. The coverage probability between the UAV and the UE, namely $P_{c,\mathrm{UAV}}(T)$, is derived as

$$\begin{aligned}
&P_{c,\mathrm{UAV}}(T)=\int\mathbb{P}(\mathrm{SNR}_{\mathrm{UAV}}>T)f_{\mathrm{UAV}}^{\mathrm{LoS}}(x)\,\mathrm{d}x\\
&=\int\mathbb{P}\left(\frac{P_tH_{x,y_{\mathrm{U}}}L^{-1}(x_0,y_{\mathrm{U}})}{N_0}>T\right)f_{\mathrm{UAV}}^{\mathrm{LoS}}(x)\mathrm{d}x\\
&\overset{(a)}{=}\int_{l_{\mathrm{U,min}}}^{l_{\mathrm{U,max}}}\mathbb{P}(H_{x_0,y_{\mathrm{U}}}>\zeta)f_{\mathrm{UAV}}^{\mathrm{LoS}}(x)\mathrm{d}x\\
&\overset{(b)}{\approx}\int_{l_{\mathrm{U,min}}}^{l_{\mathrm{U,max}}}\frac{2x(1-(1-\exp(-a\zeta))^m)}{\pi\sqrt{(l_{\mathrm{U,max}}^2-x^2)(x^2-l_{\mathrm{U,min}}^2)}}\\
&\times\exp\left(\frac{-\lambda_{\mathrm{BU}}\mathbb{E}[S_{sa}]}{\pi h_{\mathrm{U}}}\sqrt{x^2-h_{\mathrm{U}}^2}-\lambda_{\mathrm{BU}}\mathbb{E}[S_{ta}]\right)\mathrm{d}x, \quad (12)
\end{aligned}$$

where (a) is obtained by substituting $\zeta=TN_0S_{x_0,y_{\mathrm{U}}}x^{\alpha}/P_{t,u}$ and (b) follows from [12] with $a=m(m!)^{-1/m}$.

Based on (12), as the UAV's flight height increases, the probability that the UAV is located in the LoS clearance zone increases, whereas the probability of having an SNR exceeding the threshold decreases. Therefore, an optimal UAV flight height for maximizing the coverage probability of the UAV exists, which is further obtained in the following lemma.

Lemma 3. When the SNR is high enough, the maximal coverage probability is achieved at the optimal UAV's flight height given by

$$h_{\mathrm{U}}^*=\frac{-2\lambda_{\mathrm{BU}}\mathbb{E}[S_{sa}]R_{\mathrm{U}}/\pi}{\ln((\pi-2\xi)(L_{\mathrm{U}}-R_{\mathrm{U}}))-\ln((\pi+2\xi)(L_{\mathrm{U}}+R_{\mathrm{U}}))}, \quad (13)$$

where ξ is expressed as (14).

Proof: As the UAV-to-UE link is not interfered by the ground BSs, we assume that the UE's receiving SNR is high enough such that $a\zeta=m(m!)^{-1/m}\cdot\frac{TN_0S_{x_0,y_{\mathrm{U}}}x^{\alpha}}{P_t}\approx 0$ and $1-(1-\exp(-a\zeta))^m\approx 1$.

Let $t=\sqrt{x^2-h_{\mathrm{U}}^2}$. Then (12) can be rewritten as

$$P_{c,\mathrm{UAV}}(T)$$

$$\xi = \frac{\int_{L_U-R_U}^{L_U+R_U} \tan^{-1}\left(\frac{R_{\mathrm{U}}^2+L_{\mathrm{U}}^2-t^2}{\sqrt{((L_U+R_U)^2-t^2)(t^2-(L_U-R_U)^2)}}\right) \exp\left(\frac{-\lambda_{\mathrm{BU}} t}{\pi h_{\mathrm{U}}}\mathbb{E}[S_{sa}] - \lambda_{\mathrm{BU}}\mathbb{E}[S_{ta}]\right) \mathrm{d}t}{\int_{L_U-R_U}^{L_U+R_U} \exp\left(\frac{-\lambda_{\mathrm{BU}} t}{\pi h_{\mathrm{U}}}\mathbb{E}[S_{sa}] - \lambda_{\mathrm{BU}}\mathbb{E}[S_{ta}]\right) \mathrm{d}t}. \tag{14}$$

$$\begin{aligned}
&= \int_{l'_{\mathrm{U,min}}}^{l'_{\mathrm{U,max}}} \frac{2t \exp\left(\frac{-\lambda_{\mathrm{BU}} t}{\pi h_{\mathrm{U}}}\mathbb{E}[S_{sa}] - \lambda_{\mathrm{BU}}\mathbb{E}[S_{ta}]\right)}{\pi\sqrt{({l'_{\mathrm{U,max}}}^2 - t^2)(t^2 - {l'_{\mathrm{U,min}}}^2)}}\mathrm{d}t \\
&= \frac{\exp(-\lambda_{\mathrm{BU}}\mathbb{E}[S_{ta}])}{2}\left(\exp\left(\frac{-\lambda_{\mathrm{BU}}\mathbb{E}[S_{sa}]l'_{\mathrm{U,max}}}{\pi h_{\mathrm{U}}}\right)\right. \\
&\quad \left. + \exp\left(\frac{-\lambda_{\mathrm{BU}}\mathbb{E}[S_{sa}]l'_{\mathrm{U,min}}}{\pi h_{\mathrm{U}}}\right)\right) - \frac{-\lambda_{\mathrm{BU}}\mathbb{E}[S_{sa}]}{\pi^2 h_{\mathrm{U}}} \\
&\quad \times \int_{l'_{\mathrm{U,min}}}^{l'_{\mathrm{U,max}}} \tan^{-1}\left(\frac{R_{\mathrm{U}}^2 + L_{\mathrm{U}}^2 - t^2}{\sqrt{({l'_{\mathrm{U,max}}}^2 - t^2)(t^2 - {l'_{\mathrm{U,min}}}^2)}}\right) \\
&\quad \times \exp\left(\frac{-\lambda_{\mathrm{BU}} t}{\pi h_{\mathrm{U}}}\mathbb{E}[S_{sa}] - \lambda_{\mathrm{BU}}\mathbb{E}[S_{ta}]\right)\mathrm{d}t,
\end{aligned} \tag{15}$$

where $l'_{U,\mathrm{min}} = L_U - R_U$ and $l'_{U,\mathrm{max}} = L_U + R_U$ are the minimal and maximal value of variable t, respectively.

Denote $f(t) = \tan^{-1}\left(\frac{R_U^2+L_U^2-t^2}{\sqrt{(l_{U,\mathrm{max}}^2-t^2)(t^2-l_{U,\mathrm{min}}^2)}}\right)$. Note that $f(t)$ is bounded and continuous in the region $t \in [L_U - R_U, L_U + R_U]$. According to the mean value theorem for integrals, we have $\xi = f(a)$ for some $a \in [L_U - R_U, L_U + R_U]$. Then

$$\begin{aligned}
&P_{c,\mathrm{UAV}}(T) \\
&= \left(\frac{1}{2} - \frac{\xi}{\pi}\right)\exp\left(\frac{-\lambda_{\mathrm{BU}}\mathbb{E}[S_{sa}](L_{\mathrm{U}} + R_{\mathrm{U}})}{\pi h_{\mathrm{U}}} - \lambda_{\mathrm{BU}}\mathbb{E}[S_{ta}]\right) \\
&+\left(\frac{1}{2}+\frac{\xi}{\pi}\right)\exp\left(\frac{-\lambda_{\mathrm{BU}}\mathbb{E}[S_{sa}](L_{\mathrm{U}}-R_{\mathrm{U}})}{\pi h_{\mathrm{U}}}-\lambda_{\mathrm{BU}}\mathbb{E}[S_{ta}]\right).
\end{aligned} \tag{16}$$

Finally, the optimal UAV flight height is obtained by setting the derivative of (16) to zero. This completes the proof.

Note that as the UAV-to-UE link is not interfered by the ground BSs and we ignore the situation that the link was blocked by buildings, the assumption that the SNR is sufficiently high is reasonable. ■

Fig. 3 evaluates the coverage probabilities of the serving ground BSs, UAV and the total coverage probability. The system parameters are set according to Table I in Sec. V. Meanwhile, the average height of the ground BSs is set to be a tenth of the UAV's flight height. From Fig. 3, it can be observed that as the average height of the ground BSs increases, the coverage probability of ground BSs first increases to a maximal value and then decreases rapidly. This is because, when the average height of BSs exceeds that of the surrounding buildings, more BSs are located in the LoS clearance zone of the UEs, leading to increased interference among BSs, thus degrading the coverage probability of BSs. On the other hand, the coverage probability of the UAV remains close to its maximal value for a large range of flight heights, and it varies at a much slower rate than that of the coverage probability of the ground BSs. In fact, with no interference from the ground BSs, the coverage probability of the UAV degrades only due

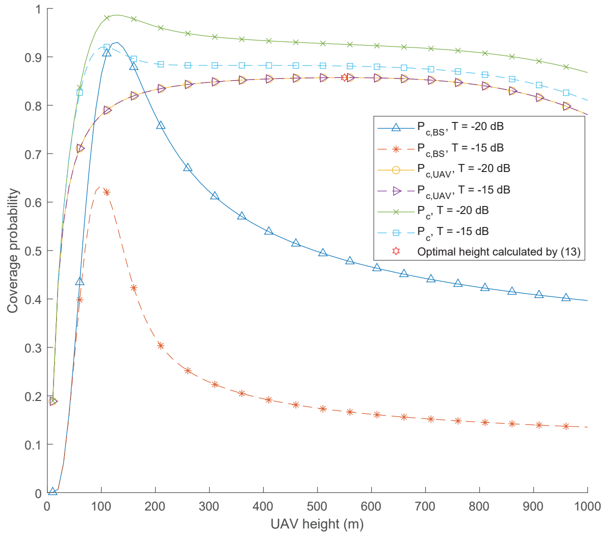

Fig. 3. The impact of UAV flight height on coverage probability.

to the increased path loss for LoS signal propagation. From Fig. 3, we also observe that, by exploiting the MC technique, the total coverage probability not only surpasses the coverage probabilities of individual BSs and UAV, but remains close to the maximum for a large range of UAV flight heights.

IV. Analysis of UE Outage Probability

In this section, we utilize a 2D Markov process to model the dynamic evolution of buffer status at the UE, and derive the UE outage probability by jointly considering the buffer state and the coverage probability derived in Sec. III. At the UE, the processes of data packets arriving into and departing from the buffer can be modeled as state transitions in a 2D Markov chain. Let (m, n) be the system state, where m and n are the number of packets received from the ground BSs and the UAV, respectively. As the UE has a finite buffer size C, we require $m + n \le C$. Fig. 4 illustrates the transition diagram of the 2D Markov Chain for $C = 5$.

Fig. 4 shows two types of state transitions, which are discussed below:

1) $(m, n) \to (m + 1, n)$ or $(m, n + 1)$: When the serving ground BS or the UAV sends a packet to the UE, with the UE's receiving SINR exceeding the given threshold, the UE can successfully receive this packet, increasing the number of packets received from the serving ground BS or the UAV in the UE buffer by one.
2) $(m, n) \to (m - 1, n)$ or $(m, n-1)$: When a packet from the ground BS or the UAV completes its service process, it is deleted from the UE buffer, decreasing the number of packets from the ground BS or the UAV in the UE buffer by one.

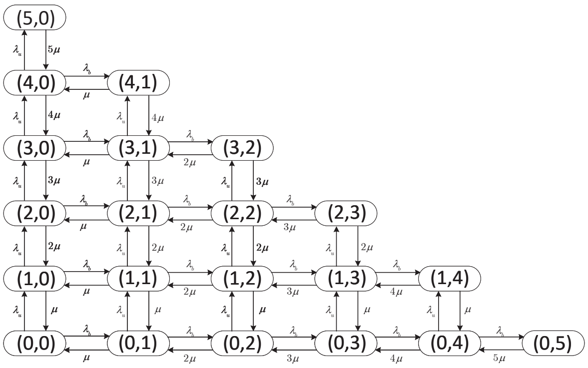

Fig. 4. Markov chain transition diagram with $C = 5$.

The 2D Markov chain as shown in Fig. 4 is reversible. Based on the Kolmogorov criteria [13], the associated stationary state distribution exists. Define $\pi(m,n)$ as the steady-state probability of the queue state (m,n). We can derive the global equilibrium equations as (17). By solving (17) at the top of the next page, the stationary state probabilities can be derived as

$$\pi(m,n) = \frac{\left(\frac{\lambda_b}{\mu}\right)^m \frac{1}{m!} \left(\frac{\lambda_u}{\mu}\right)^n \frac{1}{n!}}{\sum\limits_{\substack{0\le m+n\le C\\ m,n\ge 0}} \left(\frac{\lambda_b}{\mu}\right)^m \frac{1}{m!} \left(\frac{\lambda_u}{\mu}\right)^n \frac{1}{n!}}. \tag{18}$$

According to (18), the probability that the UE buffer is full can be derived as $\Pi_C = \sum_{i+j=C} \pi(i,j)$. Based on (11), (12) and (18), the UE outage probability is given as

$$P_{out} = 1 - (1-(1-P_{c,\mathrm{BS}})(1-P_{c,\mathrm{UAV}})) \cdot \left(1 - \frac{\left(\frac{\lambda}{\mu}\right)^C \sum\limits_{i=0}^{C} \frac{(P_{c,\mathrm{BS}})^i}{i!} \frac{(P_{c,\mathrm{UAV}})^{C-i}}{(C-i)!}}{\sum\limits_{\substack{0\le m+n\le C\\ m,n\ge 0}} \left(\frac{\lambda}{\mu}\right)^{m+n} \frac{(P_{c,\mathrm{BS}})^m}{m!} \frac{(P_{c,\mathrm{UAV}})^n}{n!}}\right). \tag{19}$$

Note that, if the S(I)NR at the UE becomes large, or the receiving threshold T becomes small, the coverage probabilities of ground BSs and UAV will approach their maximal values, $P_{c,\mathrm{BS}}^{\max}$ and $P_{c,\mathrm{UAV}}^{\max}$. Substituting them into (19), we obtain the expression of the UE outage probability when both the ground BSs and the UAV achieve their optimal coverage probabilities,

$$P_{out} = 1 - \left(1-(1-P_{c,\mathrm{BS}}^{\max})(1-P_{c,\mathrm{UAV}}^{\max})\right) \cdot \left(1 - \frac{\left(\frac{\lambda}{\mu}\right)^C \sum\limits_{i=0}^{C} \frac{\left(P_{c,\mathrm{BS}}^{\max}\right)^i}{i!} \frac{\left(P_{c,\mathrm{UAV}}^{\max}\right)^{C-i}}{(C-i)!}}{\sum\limits_{\substack{0\le m+n\le C\\ m,n\ge 0}} \left(\frac{\lambda}{\mu}\right)^{m+n} \frac{\left(P_{c,\mathrm{BS}}^{\max}\right)^m}{m!} \frac{\left(P_{c,\mathrm{UAV}}^{\max}\right)^n}{n!}}\right). \tag{20}$$

On the other hand, when the UE S(I)NR becomes small, or the receiving threshold becomes large, the coverage probability will approach zero and the resulting UE outage probability is one.

V. Simulation Results

In this section, based on the derived analytical results, the impact of several parameters on the system performance is evaluated. Unless otherwise specified, the parameters are set according to Table I.

TABLE I: Simulation parameter settings.

Carrier frequency f	32 GHz
Density of BSs λ_{BS}	$1 \times 10^{-5}/\mathrm{m}^2$
Path loss exponent α	2
Fading parameter m, shadowing $S_{x,y}$	$3, 1$
Building parameters $\mathbb{E}[W], \mathbb{E}[L], \mathbb{E}[H]$	$120, 50, 25$ m
UE height H_{UE}	1.5 m
Transmit power of BS $P_{t,b}$ and UAV $P_{t,u}$	$33, 20$ dBm
Noise power spectral density	-174 dBm/Hz
SINR threshold T	-10 dB
Density of buildings λ_{BU}	$1.7 \times 10^{-5}/\mathrm{m}^2$
UAV flight height H_{U} and radius R_{U}	$100, 100$ m
Distance between UE and UAV flight center L_{U}	300 m
Packet sent rate λ, service rate μ	$0.15, 0.01$
UE buffer size C	32

Fig. 5 evaluates the coverage probabilities of the UAV, the ground BSs, and the overall system as functions of the average height of buildings for different receiving S(I)NR thresholds. From Fig. 5 we observe that, as the average height of buildings increases, the coverage probability of the UAV monotonically decreases, whereas the coverage probability of ground BSs initially increases before decreasing. This is because, as the height of the buildings increases on average, the UAV encounters more frequent blockages from taller buildings, significantly impairing its receiving SNR. By contrast, the ground BSs may experience reduced interference from the neighboring BSs, leading to an initial increase in their coverage probability. However, as the average height of buildings further increases, the ground BSs also become obstructed by the buildings, which eventually degrades the coverage probability of the ground BSs. From Fig. 5 we also observe that, by employing the MC technique in UAV-assisted mmWave wireless networks, the total coverage probability of the system exceeds that of both the ground BSs and the UAV and, at the same time, it remains at a relatively large value unless the average height of buildings becomes significantly large.

Fig. 6 shows the total outage probability of the system as a function of the receiving S(I)NR threshold, T, for different buffer sizes at the UE. From Fig. 6 we observe that when the buffer is small, the minimum outage probability is achieved when a medium S(I)NR threshold is adopted. This is because the data packets from both terrestrial BSs and UAV arriving with high rate in the small S(I)NR threshold will be blocked due to the limitation of buffer size. However, the data packet rate of terrestrial BSs fails in a medium S(I)NR threshold and the data packets from UAV can be stored and dealt with. Then, when the buffer size is large, the minimum outage probability is achieved with a relatively small S(I)NR threshold. This is because the data packets from both terrestrial BSs and UAV with high arrival rate can be stored in the buffer and timely dealt with. When the receiving threshold becomes large, e.g. as T exceeds 40 dB, the outage probability increases, irrespective of the buffer size.

VI. Conclusion

In this paper, we analyzed the connectivity and outage probabilities of MC in UAV-assisted mmWave communication utilizing stochastic geometry theory and a Markov chain model.

$$
\begin{cases}
\pi(0,0)\cdot(\lambda_u+\lambda_b)=\pi(0,1)\mu+\pi(1,0)\mu \\
\pi(0,C)\cdot C\mu=\pi(0,C-1)\lambda_u \\
\pi(C,0)\cdot C\mu=\pi(C-1,0)\lambda_b \\
\pi(0,j)\left(j\mu+\lambda_u+\lambda_b\right)=\pi(1,j)\mu+\pi(0,j-1)\lambda_u+\pi(0,j+1)\left(j+1\right)\mu & (0<j<C) \\
\pi(i,0)\left(i\mu+\lambda_u+\lambda_b\right)=\pi(i,1)\mu+\pi(i-1,0)\lambda_b+\pi(i+1,0)\left(i+1\right)\mu & (0<i<C) \\
\pi(i,j)\left(i\mu+j\mu+\lambda_u+\lambda_b\right) \\
\quad =\pi(i-1,j)\lambda_b+\pi(i,j-1)\lambda_u+\pi(i+1,j)\left(i+1\right)\mu+\pi(i,j+1)\left(j+1\right)\mu & (0<i+j<C;i,j\neq 0) \\
\pi(i,j)\left(i\mu+j\mu\right)=\pi(i-1,j)\lambda_b+\pi(i,j-1)\lambda_u & (i+j=C;i,j\neq 0)
\end{cases}. \tag{17}
$$

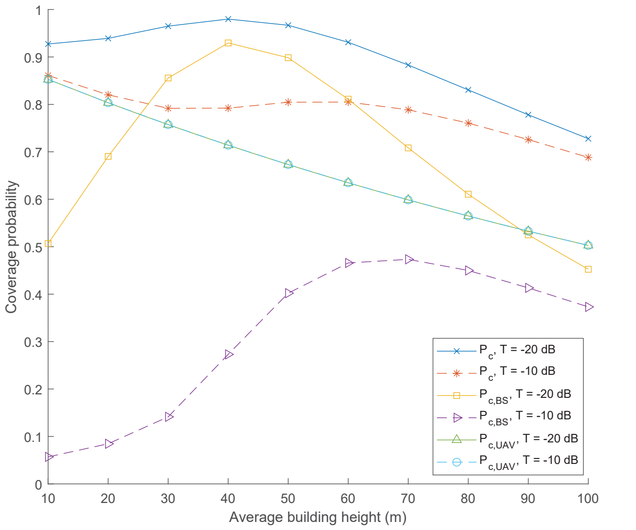

Fig. 5. Coverage probability vs. average building height.

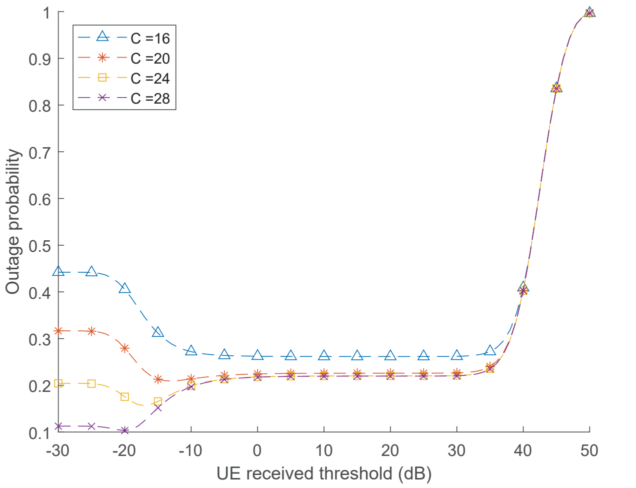

Fig. 6. UE outage probability vs. receiving S(I)NR threshold.

We derived a closed-form expression for determining the optimal flight altitude of the UAV to maximize its coverage probability. Furthermore, we demonstrate that MC enables UAVs to maintain data packet transmission even when mmWave links from terrestrial BSs fail due to medium received thresholds at UEs. Moreover, employing MC in UAV-assisted mmWave communication system can significantly improve the connectivity and communication reliability for integrated ground and aerial mmWave networks.

References

[1] M. Giordani, M. Polese, M. Mezzavilla *et al.*, "Toward 6G networks: Use cases and technologies," *IEEE Commun. Mag.*, vol. 58, no. 3, pp. 55–61, 2020.

[2] J. Struye, F. Lemic, and J. Famaey, "CoVRage: Millimeter-wave beamforming for mobile interactive virtual reality," *IEEE Trans. Wireless Commun.*, vol. 22, no. 7, pp. 4828–4842, 2023.

[3] G. Lu, J. Zhang, L. Xiang *et al.*, "A global optimization method for energy-minimal UAV-aided data collection over fixed flight path," in *ICC 2022 - IEEE Int. Conf. and Commun.*, 2022, pp. 1220–1226.

[4] C. Zhao, Y. Liu, Y. Cai *et al.*, "Non-orthogonal multiple access for UAV-Aided heterogeneous networks: A stochastic geometry model," *IEEE Transactions on Vehicular Technology*, vol. 72, no. 1, pp. 940–956, 2023.

[5] C. Chen, J. Zhang, X. Chu *et al.*, "On the optimal base-station height in mmwave small-cell networks considering cylindrical blockage effects," *IEEE Transactions on Vehicular Technology*, vol. 70, no. 9, pp. 9588–9592, 2021.

[6] V. Begishev, E. Sopin, D. Moltchanov *et al.*, "Joint use of guard capacity and multi-connectivity for improved session continuity in millimeter-wave 5G NR systems," *IEEE Trans. Veh. Technol.*, vol. 70, no. 3, pp. 2657–2672, 2021.

[7] T. Bai, R. Vaze, and R. W. Heath, "Analysis of blockage effects on urban cellular networks," *IEEE Trans. Wireless Commun.*, vol. 13, no. 9, pp. 5070–5083, 2014.

[8] D. D. Coleman and D. A. Westcott, *CWNA: Certified Wireless Network Administrator Official Study Guide: Exam PW0-105, 3rd ed.* Alameda, CA, USA: SYBEX, 2012.

[9] X. Liu, J. Xu, and H. Tang, "Analysis of frequency-dependent line-of-sight probability in 3-D environment," *IEEE Commun. Lett.*, vol. 22, no. 8, pp. 1732–1735, 2018.

[10] Y. Wang, L. Xiang, J. Zhang *et al.*, "Connectivity analysis for large-scale intelligent reflecting surface aided mmwave cellular networks," in *2022 IEEE 33rd Personal, Indoor and Mobile Radio Commun. Sympos. (PIMRC)*, 2022, pp. 432–438.

[11] A. A. Zaid, B. E. Y. Belmekki, and M.-S. Alouini, "Aerial-aided mmWave VANETs using NOMA: Performance analysis, comparison, and insights," *IEEE Trans. Veh. Technol.*, vol. 73, no. 4, pp. 4742–4758, 2024.

[12] T. Bai and R. W. Heath, "Coverage and rate analysis for millimeter-wave cellular networks," *IEEE Trans. Wireless Commun.*, vol. 14, no. 2, pp. 1100–1114, 2015.

[13] F. P. Kelly, *Reversibility and Stochastic Network.* Wiley, 1979.